Polymer 50 (2009) 5390–5397

Contents lists available at ScienceDirect

Polymer

journal homepage: www.elsevier.com/locate/polymer

Chemical modification of PP architecture: Strategies for introducing long-chain branching

Khalil El Mabrouk [a], J. Scott Parent [a,*], Bharat I. Chaudhary [b], Ronjuan Cong [c]

[a] Department of Chemical Engineering Queen's University, Kingston, ON, Canada K7L 3N6
[b] The Dow Chemical Company, 171 River Road, Piscataway, NJ 08854, USA
[c] The Dow Chemical Company, 2301 Brazosport Blvd, Freeport, TX 77541-3257, USA

ARTICLE INFO

Article history:
Received 14 July 2009
Received in revised form
21 September 2009
Accepted 26 September 2009
Available online 1 October 2009

Keywords:
Polypropylene
Long-chain branching
Rheology

ABSTRACT

Two strategies for introducing long chain branching (LCB) to a polypropylene homopolymer (PP) are evaluated in terms of the product's molecular weight and branching distributions, and in terms of melt-state shear and extensional rheological properties. Single step processes involving radical-mediated addition of PP to triallyl phosphate are shown to generate bimodal products with highly differentiated chain populations, while a two step sequence involving PP addition to vinyltriethoxysilane followed by moisture-curing is shown to generate more uniform architectures. As a result, the sequential approach can improve low-frequency shear viscosity and extensional strain hardening characteristics while staying below the polyolefin's gel point. The composition and molecular weight distribution transformations that underlie sequential LCB techniques are discussed.

1. Introduction

The linear structure of commercial polypropylene (PP) homopolymers is ill-suited for melt-state processing operations that impose extensional deformations [1]. This can be corrected by generating a long-chain branch (LCB) architecture through chemical modification [2,3], and although a wide range of chemistry can be brought to bear on the problem, free radical methods are generally favoured, since they can activate C–H bonds under solvent free conditions in the presence of atmospheric moisture and oxygen [4,5]. Of particular interest are LCB techniques that are amenable to short residence time, reactive extrusion conditions [6].

Two general strategies for preparing LCB-PP are illustrated in Scheme I. The simplest method involves the peroxide-initiated grafting of multi-functional coagents such as triallyl phosphate (TAP). This single-step process involves simultaneous PP fragmentation and cross-linking, the balance of which controls the length, frequency, and distribution of branches. The melt-state rheology of these derivatives have been studied under steady shear [7,8], oscillatory shear [9,10], and extensional deformations [9,11], and a wide range of coagent systems been proven capable of generating long-chain branching characteristics from a linear PP homopolymer. We have recently characterized the bimodal architecture of these LCB products [12], and correlated this knowledge of polymer structure to melt-state rheological properties [13]. A greater appreciation of the merits and limitations of a coagent-based approach has led us to consider alternate strategies, in hope of achieving more uniform branching and molecular weight distributions.

The sequential approaches illustrated in Scheme I draw upon conventional thermoset chemistry, in which a polyolefin is functionalized by radical graft modification, and then cross-linked to below the gel point using non-radical methods [14,15]. This strategy sacrifices the convenience of a single-step modification to gain independent control over the chain scission incurred during PP functionalization and the molecular weight growth needed to generate a branched architecture. In one case, PP is functionalized by peroxide-initiated addition to vinyltriethoxysilane (VTES) [16], giving a PP-g-VTES derivative that can be moisture-cured into a LCB material [17,18]. A second variation involves maleation to give PP-g-MAn, which can be cross-linked by multi-functional primary amines [19,20].

In spite of the aforementioned reports of LCB-PP synthesis by sequential grafting-crosslinking techniques, the architecture and rheological properties of these derivatives remains poorly understood. Our objective was to prepare uniformly branched, gel-free LCB-PP materials that demonstrate exceptional melt strength and extensional strain hardening characteristics. This report describes successful examples of the silylation and maleation techniques, using spectroscopy, triple-detector gel permeation chromatography, and melt-state rheology to characterize LCB-PP derivatives.

* Corresponding author. Tel.: +613 533 6266; fax: +613 533 6637.
E-mail address: parent@chee.queensu.ca (J.S. Parent).

0032-3861/$ – see front matter © 2009 Elsevier Ltd. All rights reserved.
doi:10.1016/j.polymer.2009.09.066

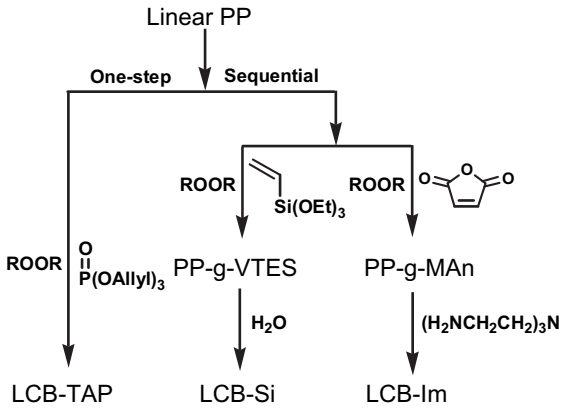

Scheme I. Strategies for PP Branching.

The composition and molecular weight distribution transformations that underlie effective LCB syntheses are discussed.

2. Experimental section

2.1. Materials

An additive-free grade of PP homopolymer (M_n of 55.1 kg/mol and a polydispersity of 5.4) was used throughout this work. Butyl lithium (2.0 M in hexanes), dicumyl peroxide (DCP, 98%), maleic anhydride (MAn, 99%) tris(2-aminoethyl)amine (TAEA, 96%) and vinyl triethoxysilane (VTES, 97%) were used as received from Sigma Aldrich, while dibutyltin dilaurate (DBTDL, 98%, Alfa Aesar) was similarly used without purification.

2.2. PP-g-TAP

PP powder (3.5 g) was tumble-mixed with a solution of DCP (7 mg, 0.2 wt%) in TAP (0.07 g, 2 wt%) for 20 min. This mixture was reacted for 5 min under a nitrogen atmosphere within a recirculating, twin screw mini-extruder (DSM-5, DSM Research-Netherlands) at 180 °C and a screw speed of 60 rpm, giving PP-g-TAP.

2.3. PP-g-VTES

PP powder (3.5 g) was tumble-mixed with a solution of DCP (7 mg, 0.2 wt%) in VTES (0.175 g, 5 wt%) for 20 min. This mixture was reacted for 5 min under a nitrogen atmosphere within a recirculating, twin screw mini-extruder at 180 °C and a screw speed of 60 rpm, giving PP-g-VTES. PP-g-VTES samples for graft content analysis were purified from residual VTES by dissolving in refluxing xylene, precipitating from acetone, and drying under vacuum at 60 °C. Grafted VTES contents were calculated from FT-IR spectrum integrations of the 1064–1094 cm^{-1} absorbance of the silane relative to a 422–496 cm^{-1} internal standard region originating from PP. Calibration standards for this FT-IR method were prepared by melt mixing known quantities of ethyltriethoxysilane to purified starting material.

PP-g-VTES samples for GPC analysis were rendered inert by treatment with BuLi. A solution of PP-g-VTES (0.5 g) in dry xylene (35 ml) was backfilled with nitrogen and heated to reflux prior to the drop-wise addition of excess BuLi (1 ml, 2.5 M in hexane). The solution was refluxed for 3 h prior to injecting aqueous NH_4Cl (2 ml, saturated) and recovering the polymer by precipitation into acetone and drying under vacuum at 60 °C.

2.4. LCB-Si

PP-g-VTES (1 g) were stabilized with 500 ppm Irganox-1010, 1000 ppm Irgafos-168 and 600 ppm calcium stearate and moisture-cured by melt-mixing DBTDL (5 μL) into thin films, and immersing in boiling water for 15 h. The films were dried under vacuum at 60 °C, giving the branched derivatives LCB-Si.

2.5. PP-g-MAn

PP powder (3.5 g) was tumble-mixed with a 2 ml of chloroform solution containing the desired amounts of DCP and MAn. The resulting mixture was reacted for 5 min under a nitrogen atmosphere within a recirculating twin screw extruder at 180 °C and a screw speed of 60 rpm, giving PP-g-MAn. All PP-g-MAn samples were purified from residual MAn by dissolving in refluxing xylene, precipitating from acetone, and drying under vacuum at 60 °C. Grafted MAn contents were calculated from FT-IR spectrum integrations of the area derived from the 1754–1808 cm^{-1} C=O anhydride absorbance relative to a 422–496 cm^{-1} internal standard region originating from PP. Calibration standards for this FT-IR method were prepared by melt mixing known quantities of 1-dodecenylsuccinic anhydride to purified starting material.

2.6. LCB-Im

Purified PP-g-MAn samples for amine-curing were stabilized with 500 ppm Irganox-1010, 1000 ppm Irgafos-168 and 600 ppm calcium stearate. Cross-linking of ground, stabilized PP-g-MAn (3.5 g) was accomplished by casting a chloroform solution containing 0.33 molar equivalents of TAEA relative to the anhydride content of the sample. The powder was tumble-mixed to remove residual chloroform, and the resulting masterbatch was reacted in a twin screw extruder at 180 °C, 60 rpm for 5 min, giving LCB-Im.

2.7. Instrumentation and analysis

FT-IR spectra of purified films were acquired with a Nicolet Avatar 360 FTIR ESP instrument. High temperature triple detection GPC analysis was conducted in 1,2,4-trichlorobenzene (TCB) at 150 °C and 1 ml/min using a Polymer Labs PL 220 detector equipped with a Precision Detectors (Model 2040) light scattering instrument, for which the 15° angle detector was used for calculation purposes. The viscometer was a Viscotek model 210R detector. The column bank consisted of four 7.8 × 300 mm PL gel 20 micron Mixed A beds. The dn/dc value used for calculating molecular weights from the light scattering data was 0.104 mL/g. The detector responses were calibrated using an internally validated polyethylene standard. The samples were dissolved in 2,6-di-*t*-butyl-4-methylphenol (BHT) stabilized TCB at 160 °C for approximately 2.5 h and filtered prior to analysis.

The insoluble material content of LCB-PP samples was determined by extracting cured products with refluxing xylenes from 120 mesh sieve cloth. Extraction solutions were stabilized with 100 ppm of BHT, and the procedure was conducted for a minimum of 2 h, with longer times having no effect on the results. Unextracted material was dried under vacuum to constant weight, with insoluble content reported as a weight percent of the original LCB-PP sample.

Samples for rheological analysis were stabilized with 500 ppm Irganox-1010, 1000 ppm Irgafos-168 and 600 ppm calcium stearate. Oscillatory elastic (G′) and loss (G″) moduli were measured under a nitrogen atmosphere using a Reologica ViscoTech controlled stress rheometer equipped with 20 mm diameter parallel plates. The instrument was operated at 180 °C with a gap of 1 mm over

Table I
Properties of unmodified PP, functionalized PP, and LCB-PP materials.

			Functionalized PP derivatives						LCB derivatives			
Expt.	[DCP] μmole/g	[Modifier] mmole/g	Graft Yield mmole/g	Peroxide Yield[a] mol/mol	M_n kg/mol	M_w/M_n	Average grafts per chain	η_o kPa·s	Insoluble material wt%	M_n kg/mol	M_w/M_n	η_o kPa·s
A.	Unmodified		–	–	55.1	5.4	–	2.2	–	–	–	–
B.	TAP								LCB-TAP			
	7.4	0.09	–	–	–	–	–	–	5.0	29.9[b]	5.6[b]	8.4
	VTES		PP-g-VTES						LCB-Si			
C.	7.4	0.26	0.038	2.6	28.6	3.5	1.1	0.4	0.1	37.1	10.5	38.6
D.	18.5	0.26	0.073	2.0	22.3	3.5	1.7	0.2	12.0	27.6[b]	9.0[b]	N/A
	MAn		PP-g-MAn						LCB-Im			
E.	1.9	0.05	0.035	9.4	38.1	4.4	1.3	1.4	0.7	32.0	4.0	13.4
F.	3.7	0.05	0.051	6.9	37.7	3.6	1.9	0.8	1.6	31.2[b]	3.9[b]	N/A

[a] moles of grafted modifier/mole of initiator-derived cumyloxyl radicals.
[b] Gel-free, xylene-soluble fraction only.

frequencies 0.04–188 rad/s. Stress sweeps were acquired to ensure that all data were acquired within the linear viscoelastic regime. Creep and creep-recovery experiments were performed using the aforementioned instrument at 180 °C using a stress of 10 Pa. Extensional viscosity data were acquired at 180 °C using an SER Universal Testing Platform from Xpansion Instruments.

3. Results

3.1. LCB-TAP

The isotactic PP used throughout this work was an additive-free homopolymer with an M_n of 55.1 kg/mol and a polydispersity of 5.4. Heating this material with dicumyl peroxide (DCP) and TAP to 180 °C gave a LCB-TAP derivative with the structural features listed in Table 1 (Expt. B). The reaction raised the molecular weight of a small population of chains, with 5 wt% of LCB-TAP reaching the gel point. The remaining 95 wt% of LCB-TAP was soluble in hot xylene and trichlorobenzene, and could be subjected to gel permeation chromatography (GPC). The absolute molecular weight distributions plotted in Fig. 1a show that the dominant chain population within LCB-TAP had a lower M_n than its parent material (Table I). Furthermore, Mark-houwink plot (ln ([η]) versus log(MW)) of this fraction overlaid well with linear unmodified PP(Fig. 1b). Only a small amount of branched product in the 10^7–10^9 molecular weight range was evident in the MWD of extracted LCB-TAP. As a result, the polydispersity of this extract fraction of LCB-TAP ($M_w/M_n = 5.6$) was only marginally greater than that of the starting material ($M_w/M_n = 5.4$).

This bimodal architecture results from the different susceptibility of two chain populations with respect to fragmentation and crosslinking. The scission of linear chains yields low-mass fragments that are statistically less susceptible to coagent-assisted crosslinking, while the crosslinking of linear chains produces branched material

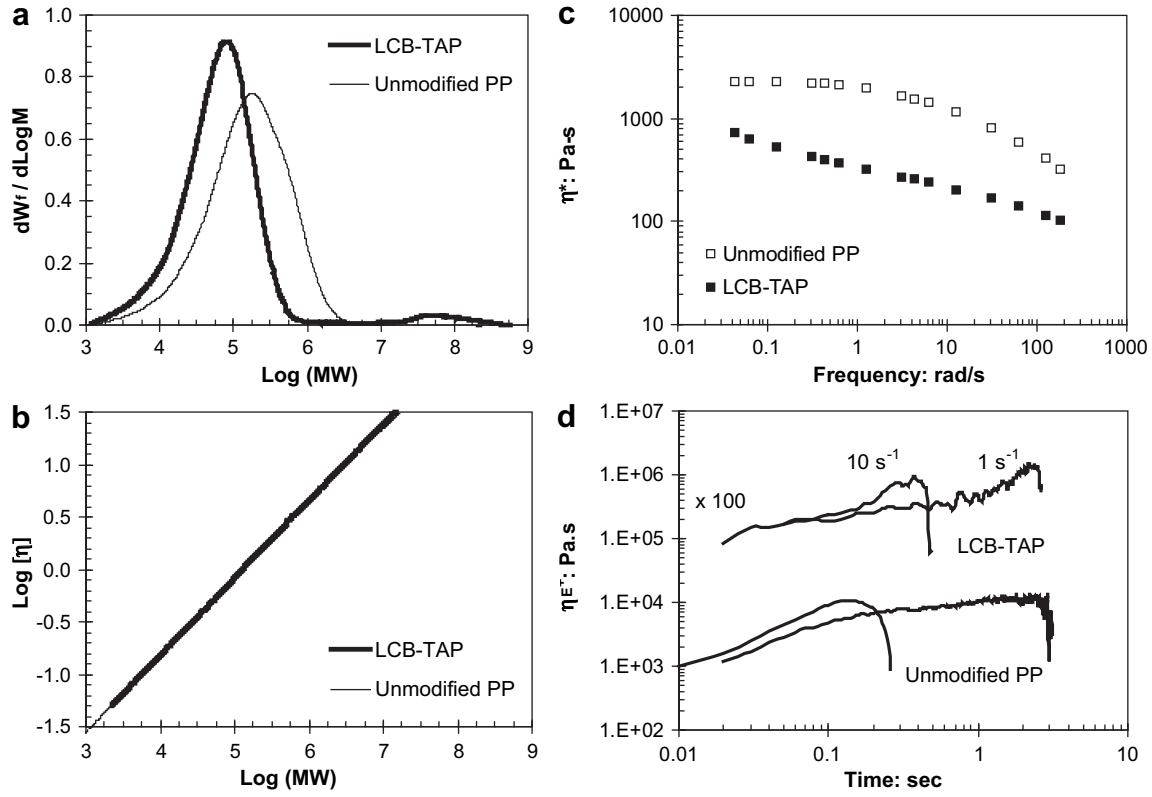

Fig. 1. GPC analysis of the soluble components of PP and LCB-TAP and melt-state rheological analysis of unfractionated materials.

whose architecture becomes more resistant to size reduction by macro-radical fragmentation as its degree of branching increases. Therefore, single-step coagent-based methods of introducing long-chain branching to PP yield bimodal molecular weight and branching distributions [11,12].

In spite of their non-uniformity, LCB-TAP products can provide useful melt flow properties, as illustrated by the rheological data plotted in Fig. 1c,d. Dynamic shear viscosities (η^*) recorded for the unfractionated LCB-TAP sample containing 5 wt% gel were lower than those of unmodified PP throughout the observable frequency range (Fig. 1c), even though the zero-shear viscosity of the branched product was nearly four times greater (Table I). Clearly, entanglement effects derived from the branched chain population within LCB-TAP were intense enough to suppress Newtonian behaviour in a dynamic shear measurement [10,21], and to introduce a small measure of extensional strain hardening character that is absent in its unmodified precursor (Fig. 1d) [22].

3.2. LCB-Si

Notwithstanding the potential utility of TAP-based LCB-PP products, practical methods of generating more uniform branching distributions are expected to have equal or greater commercial value. One such strategy exploits the robust nature of radical PP modifications to generate a trialkoxysilane derivative, PP-g-VTES, that can be moisture-cured to produce a branched product (LCB-Si; Scheme 1). As noted above, chain scission is unavoidable when PP is activated with peroxides [23]. However, by decoupling the chain scission incurred during PP functionalization from the cross-linking process that builds molecular weight and branching, the bimodality that is inherent to coagent-based techniques may be avoided.

Reaction of PP with 0.2 wt% DCP and 5 wt% VTES (Expt. C, Table I) resulted in substantial M_n and polydispersity reductions. This is consistent with the principles of controlled PP degradation, in which high molecular weight chains are statistically more likely to engage in hydrogen atom abstraction, thereby leading to a disproportionate amount of macro-radical scission compared to smaller chains within the distribution [24]. Radical degradation was accompanied by the grafting of 0.7 wt% VTES (0.037 mmole/g), which for a polymer of $M_n = 28.6$ kg/mol, amounts to an average of 1.1 trialkoxysilane groups for each chain within PP-g-VTES-C.

Lewis acid catalyzed moisture curing [25] of PP-g-VTES-C gave a branched derivative, LCB-Si-C, that was completely soluble in boiling xylene – FT-IR analysis of the 0.1 wt% of extraction residue revealed no evidence of PP. The expected increase in M_n brought on by the cross-linking of pendant silane groups was accompanied by an increase in polydispersity from 3.5 to 10.5 (Expt, C, Table I). The light scattering data plotted in Fig. 2a, and the molecular weight distributions plotted in Fig. 2b, show that moisture-curing raised the molecular weight of a significant fraction of PP-g-VTES chains, but had no substantial affect on the majority chain population.

We suggest that the non-uniform cure performance of PP-g-VTES-C is the result of a non-uniform distribution of silane grafts. Whitney and coworkers have demonstrated the repeated functionalization of vinylsilane-grafted hydrocarbons [26,27], showing that monomer oligomerization is not problematic, but intramolecular hydrogen atom transfer, followed by monomer addition to resulting alkyl radical adduct can be significant (Scheme II). These radical translocations place multiple silane grafts in close proximity, unlike the intermolecular hydrogen transfers that shift grafting activity to a different polyolefin chain. The importance of intramolecular hydrogen transfer to PP oxidation is well established [28], and its effect in the PP-g-VTES system would be to skew composition distributions such that some chains possessed more than 1.1 grafts, while others remained unfunctionalized.

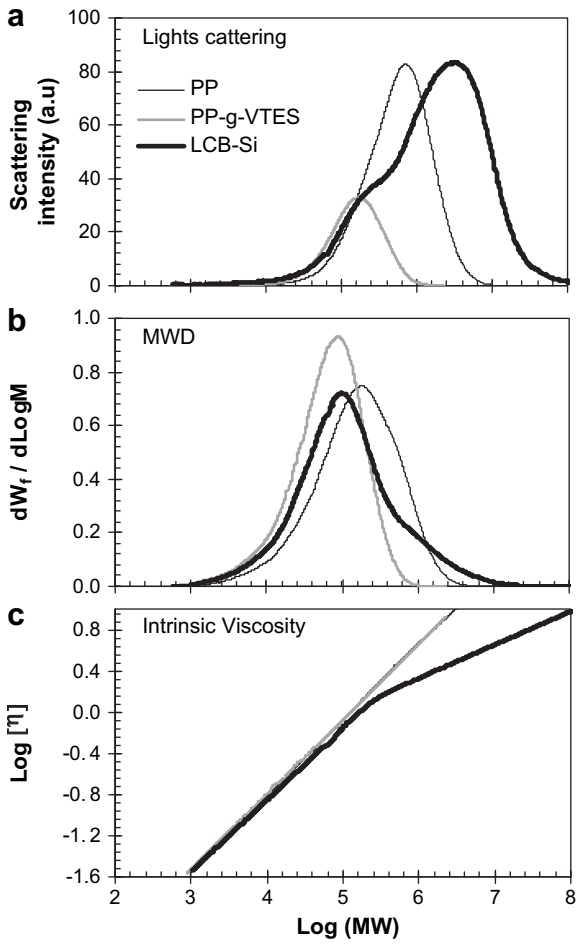

Fig. 2. GPC data for unmodified PP and its PP-g-VTES-C and LCB-Si-C derivatives (Expt. C, Table I).

The Mark-Houwink plots presented in Fig. 2c provide further insight into the structure of LCB-Si derivatives. Whereas unmodified PP and PP-g-VTES generated linear double-log plots of $[\eta]$ versus MW, LCB-Si–C demonstrated significant curvature beyond $M_w = 10^5$. This is unambiguous evidence of branching within moisture-cured chains, which produce a lower solution viscosity than a linear polymer of equivalent molecular weight. The intrinsic viscosities of low molecular weight LCB-Si–C material were depressed slightly, indicating that some branching existed within this chain population. Taken together, the GPC data show that silylation/moisture curing does not give unimodal branching distributions, but it can provide much greater uniformity than a single-step coagent-based technique.

The rheological data presented in Fig. 3 demonstrates the benefits derived from the more balanced branching distribution produced by the LCB-Si approach. Unmodified PP and PP-g-VTES-C exhibited melt flow properties that are consistent a linear structure. Both materials reached a terminal flow condition, with G′ scaling with ω^2 below 0.13 rad/s for PP and 0.44 rad/s for its silylated derivative. In contrast, the moisture-cured sample, LCB-Si–C, showed no evidence of a Newtonian plateau, as G′ did not enter the terminal region within the observable frequency range. Branch entanglements were equally influential under extensional deformations, as LCB-Si–C exhibited strong, progressive strain hardening to a comparatively high elongation (Fig. 3c). Creep compliance analysis produced a steady-state viscosity measurement of 38.6 kPa s within 1000 s, after which a substantial elastic recovery was observed (Fig. 3d).

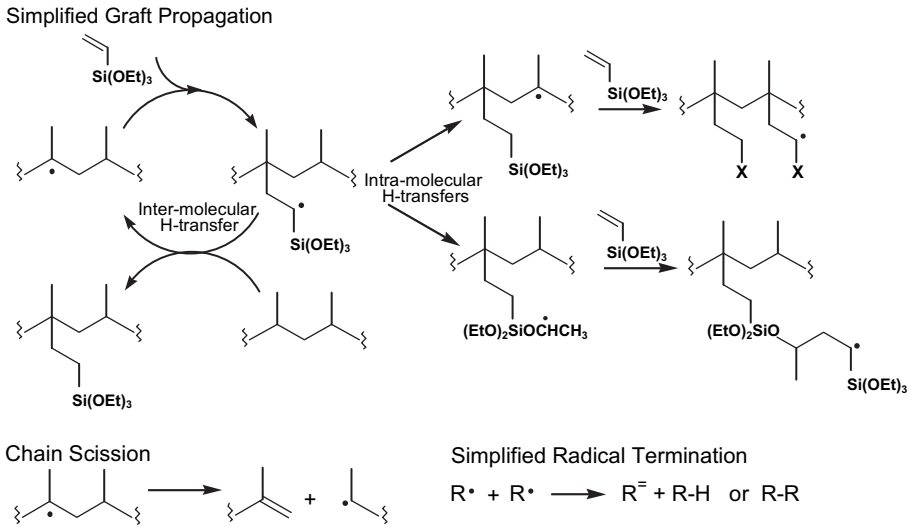

Scheme II.

In an effort to generate branching amongst the entire population of LCB-Si chains, we increased the amount of bound VTES by raising the concentration of initiator (low monomer conversions meant that VTES availability was not a limiting factor). This gave sample PP-g-VTES-D, whose VTES content of 1.4 wt% and M_n of 22.3 kg/mol amounted to an average of 1.7 silane grafts per chain (Table I). Although these measures might indicate that a greater fraction of PP chains were affected by radical activity, moisture-curing produced 12 wt% gel along with 88 wt% of xylene-soluble matrix material whose M_n was just 27.6 kg/mol. By all accounts the branching distribution of LCB-Si-D was as divergent as that of LCB-TAP, and the sample's rheological properties reflect this architecture. High-frequency η^* values for unfractionated LCB-Si-D were less than those of the parent material (Fig. 4a), owing to a relatively low matrix molecular weight, whereas low-frequency values were dominated by the entanglement effects imposed by the sample's gel fraction. No steady-state could be achieved within 1000 s of a creep compliance test, and the sample demonstrated extensive strain hardening when subjected to an extensional deformation (Fig. 4b).

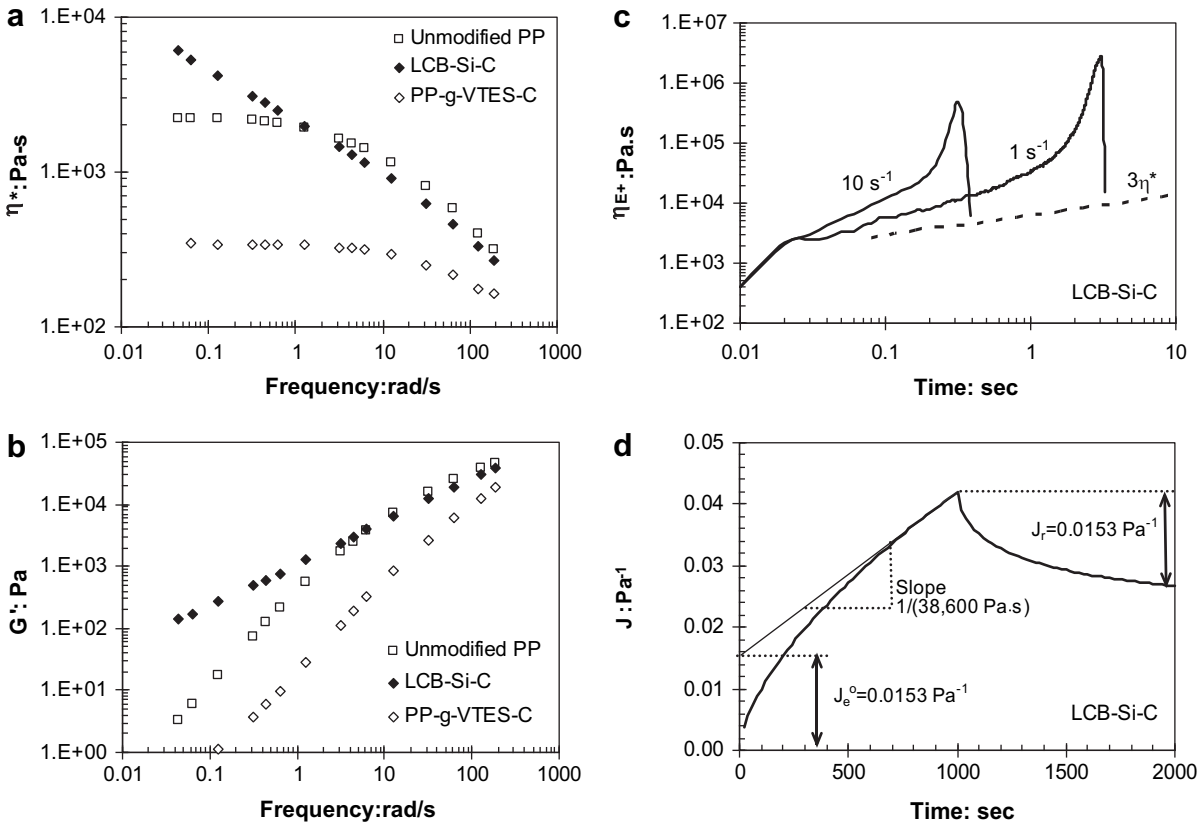

Fig. 3. Rheological data for unmodified PP and its PP-g-VTES-C and LCB-Si-C derivatives (Expt. C, Table I).

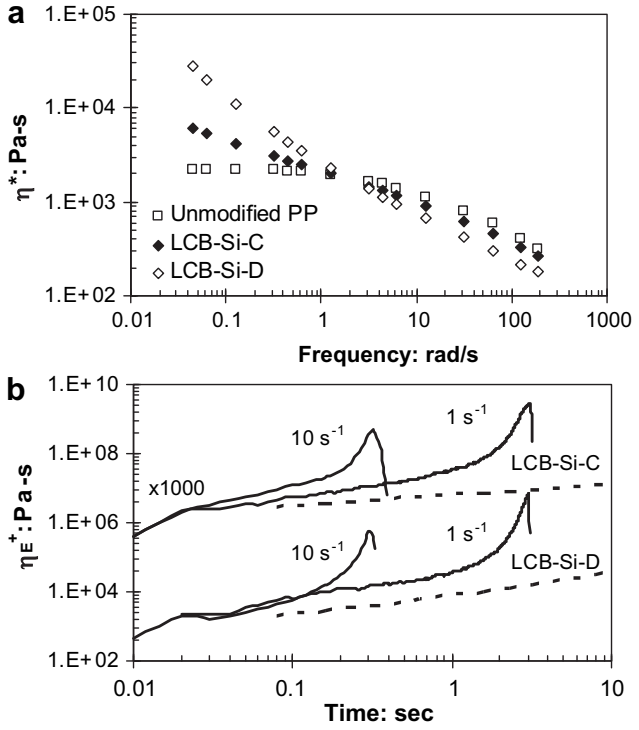

Fig. 4. Rheolgical data for unmodified PP, LCB-Si-C, and LCB-Si-D.

3.3. PP-Im

A variation of the silane-grafting/moisture-curing approach to PP branching involves free radical grafting of maleic anhydride to yield PP-g-MAn, followed by reaction with tris(2-aminoethyl)amine (TAEA) to give a branched imide derivative, LCB-Im (Scheme I). The data summarized in Table I show that maleation requires relatively small reagent loadings to generate an average of one functional group per PP chain. Whereas peroxide yields did not exceed 3.0 moles of grafted VTES per mole of initiator-derived radicals, those recorded for maleation ranged from 6.9 mol/mol (where all monomer was consumed) to 9.4 mol/mol. This means that less peroxide is needed to achieve grafting targets, which in turn reduces the extent of polymer degradation. Our PP-g-MAn derivatives had M_n values on the order of 40 kg/mol, and anhydride contents averaging 1.4 to 1.9 grafts per chain.

Knowledge of the anhydride content of PP-g-MAn samples was used to deliver 0.33 equivalents of TAEA for solvent-free crosslinking to give branched materials containing small gel contents (Table 1). Fig. 5 presents GPC data on soluble fractions, which reveals the effect of PP-g-MAn-E imidation on molecular weight distribution and product architecture. Unlike the VTES system, functional group activation did not raise the molecular weight of the graft-modified materials, but resulted in a slight overall decline. This chain scission is expected for high-temperature PP processing, but its impact on molecular weight should have been outweighed by the chain growth generated by triamine crosslinking. However, light scattering and intrinsic viscosity data (Fig. 5a and c, respectively) show that branching was restricted to chains with molar masses greater than 500 kg/mol, and was concentrated within a small chain population with molecular weights in the 1500–8000 kg/mol range. Only a small fraction of PP-g-MAn was converted to branched material, yielding a product similar to that generated by a single-step TAP grafting process. Continued research into the distribution and structure of the anhydride functionality introduced to PP-g-MAn is needed to understand the origin of this non-uniform branching architecture [29].

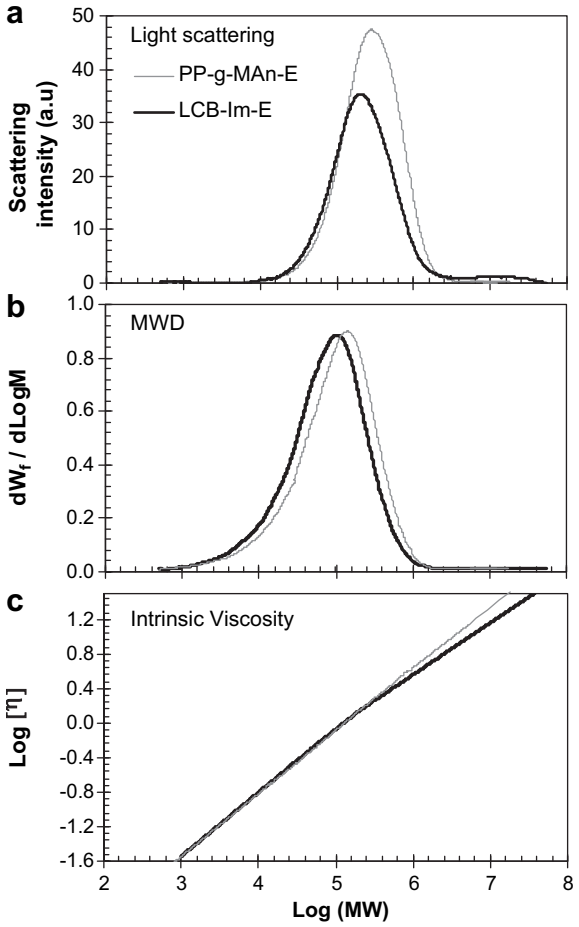

Fig. 5. GPC data for PP-g-MAn-E and LCB-Im-E derivatives (Expt. E, Table I).

The melt-state rheological properties of unfractionated LCB-Im derivatives are presented in Fig. 6. Under oscillatory shear deformations, the complex viscosity of both LCB-Im derivatives exceeded that of the parent material (Fig. 6a,b), with greatest differences observed at low frequencies where branch entanglement effects are most influential. The milder reagent loading (Expt E; Table I) yielded a lightly branched LCB-Im derivative that exhibited good extensional properties (Fig. 6c) and a small degree of elastic recovery following a creep measurement (Fig. 6d). The higher peroxide loading used in Experiment F converted all MAn to polymer bound grafts, while subsequent imide curing gave a small gel content. This product, LCB-Im-F, demonstrated higher η^* values at low frequencies, but did not exhibit greater extensional strain hardening characteristic than its gel-free analogue, LCB-Im-E.

4. Discussion

The sequential approach to LCB synthesis involves two distinct transformations of polymer composition and molecular weight (Scheme III). The first transformation, monomer grafting, operates on a PP homopolymer's molecular weight distribution to create a joint distribution of molecular weight and composition. The resulting silylated or maleated derivative will have a discrete graft content distribution (0, 1, 2, 3, etc grafts per chain), with each member having a continuous molecular weight distribution that may, or may not, be unique. Relatively little is known about this

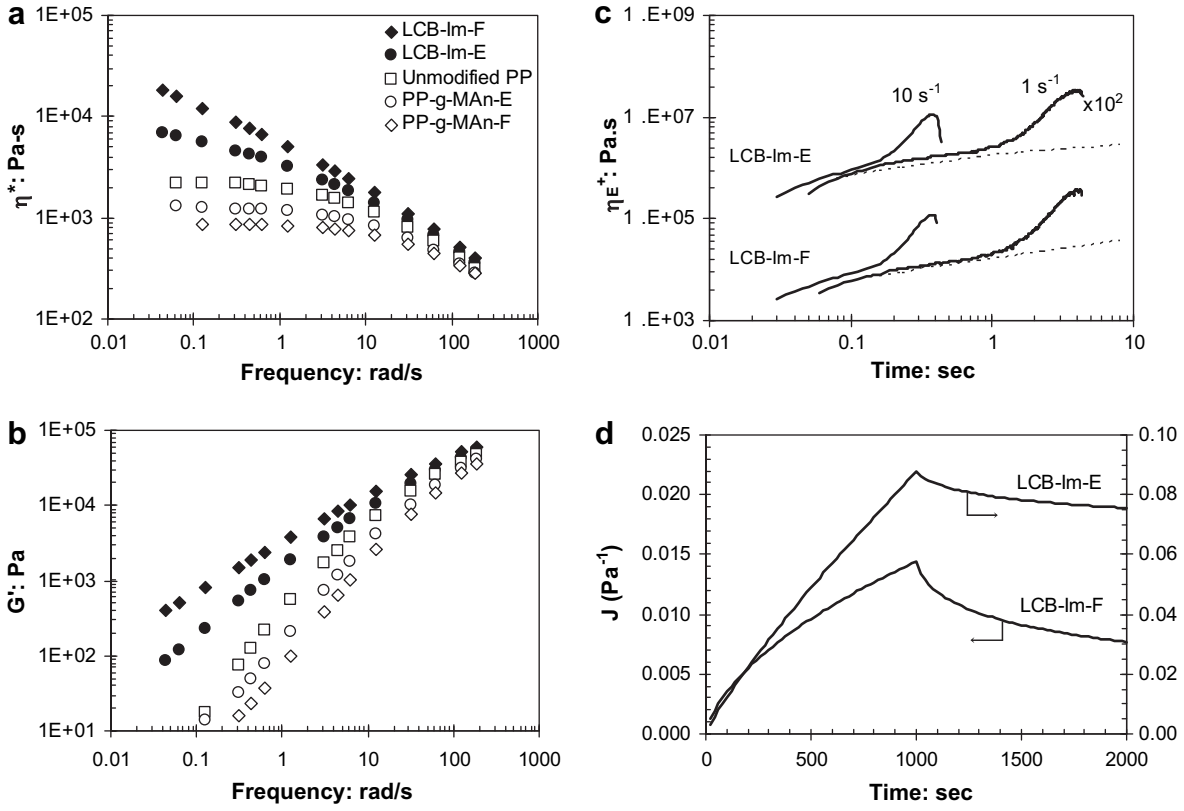

Fig. 6. Rheological data for unmodified PP, PP-g-MAn and LCB-Im derivatives.

joint distribution, since only the overall MWD is experimentally observable. Nevertheless, the data presented in this report provide some insight into the structure of PP-g-VTES and PP-g-MAn.

The distribution of silane grafts within PP-g-VTES is such that some chains remain unmodified while others are multiply-grafted. This condition would seem to be unavoidable, since the kinetic chain length of graft propagation, and the frequency of intermolecular hydrogen atom transfer events that distributes grafts amongst polymer chains, is not sufficiently competitive with PP fragmentation (Scheme II). Indeed, the silylation conditions used in this work may have functionalized all PP chains were it not for macro-radical scission continually increasing their number.

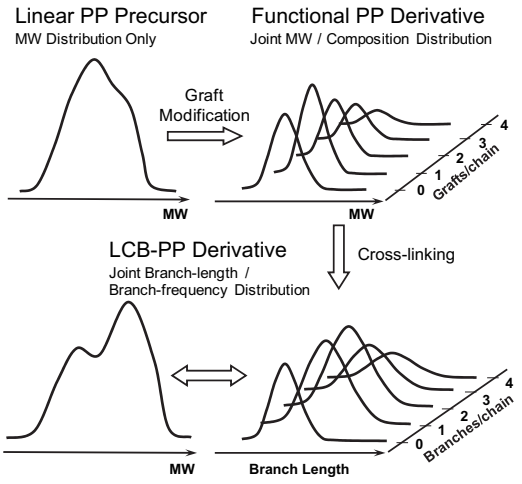

Scheme III.

The second transformation of a sequential LCB synthesis involves cross-linking by functional group activation. This process acts upon the joint MW-composition distribution of the functional PP derivative to create a new joint distribution; one between branch length and branch frequency (Scheme III). Branch lengths are dictated by the molecular weight distribution of PP-g-VTES and PP-g-MAn, while the number of branches per LCB chain depends on the structure of graft-modified materials, the functionality of the cure system employed, and the extent of silane/anhydride conversion.

Since the unfunctionalized material within PP-g-VTES is not transformed by moisture-curing, it will comprise a linear chain population within LCB-Si with a molecular weight distribution that was established during graft modification. Any PP-g-VTES chain containing one or more alkoxysilane groups can contribute its molecular weight to a branched structure by engaging in hydrolysis/condensation chemistry. While it is relatively easy to estimate average branch lengths from the molecular weight distribution of PP-g-VTES, it is very difficult to predict how many silane groups will form a common branch point, since moisture-curing is a non-stoichiometric reaction. As a result of this uncontrolled nature, the branching frequencies within LCB-Si derivatives are difficult to estimate.

The transformation of PP-g-MAn into LCB-Im is more predictable, since aminolysis of the cyclic anhydride and the subsequent dehydration of the acid-amide intermediate gives the desired imide with a 1:1 anhydride:amine stoichiometry. Therefore, the functionality of the amine cross-linking reagent (diamine, triamine, tetraamine, etc) will dictate the maximum number of anhydride groups that can form a common branch point. For example, a PP-g-MAn sample with a uniform distribution of one anhydride graft per chain could, upon cross-linking with a reagent such as hexamethylenediamine, engage two chains at each branch point, whereas the triamine applied in this work has the potential to link three

chains. Depending on the placement of anhydride groups relative to one another, chains containing multiple anhydride grafts can provide more expansive branched architectures with molecular weights several times those found in PP-g-MAn. In such cases, it may be difficult to avoid the gel point.

5. Conclusions

Sequential functionalization/cross-linking strategies can create more uniform branching distributions than single-step, coagent-based techniques. The joint molecular weight-composition distribution established by the initial grafting process dictates the extent to which a given chain can be incorporated into a branched network, and the branch length that it can contribute. Appropriate control of graft contents and cure efficiencies can provide favourable rheological properties in the absence of a gel fraction.

References

[1] Stange J, Uhl C, Munstedt H. J Rheology 2005;49:1059–79.
[2] Weng W, Hu W, Dekmezian AH, Ruff CJ. Macromolecules 2002;35:3838–43.
[3] Jorgensen JK, Redford K, Ommundsen E, Stori A. J Appl Polym Sci 2007;106:950–60.
[4] Russell KE. Prog Polym Sci 2002;27:1007–38.
[5] Lugao AB, Artel BWH, Yoshiga A, Lima LFCP, Parra DF, Bueno JR, et al. Rad Phys Chem 2007;76:1691–5.
[6] Liu NC, Baker WE. Adv Polym Tech 1992;11:249–62.
[7] Kim BK, Kim KJ. Adv Polym Technol 1993;12:263–9.
[8] Wang X, Tzoganakis C, Rempel GL. J Appl Polym Sci 1996;61:1395–404.
[9] Nam GJ, Yoo JH, Lee JW. J Appl Polym Sci 2005;96:1793–800.
[10] Borsig E, van Duin M, Gotsis AD, Picchioni F. Eur Polym J 2008;44:200–12.
[11] Tian J, Yu W, Zhou C. Polymer 2006;47:7962–9.
[12] Parent JS, Sengupta SS, Kaufman M, Chaudhary BI, Poche D, Cousteaux S. Polymer 2009;50:85–94.
[13] Parent JS, Bodsworth A, Sengupta SS, Kontopoulou M, Chaudhary BI. Polymer 2008;49:3884–91.
[14] Yang S, Song G, Zhao Y, Yang C, She X. Polym Eng Sci 2007;47:1004–8.
[15] Ohnishi R, Fujimura T, Tsunori R, Sugita Y. Macromol Mater Eng 2005;290:1227–34.
[16] Nachtigall SMB, Stedile FC, Felix AHO, Mauler RS. J Appl Polym Sci 1999;72:1313–9.
[17] Beltrán M, Mijangos C. Polym Eng Sci 2000;40:1534–41.
[18] Wang Z, Wu X, Gui Z, Hu Y, Fan W. Polym Int 2005;54:442–7.
[19] Kim KY, Kim SC. Macromol Symp 2004;214:289–97.
[20] Koster M, Hellman GP. Macromol Mater Eng 2001;286:769–73.
[21] Kurzbeck S, Oster F, Münstedt H, Nguyen TQ, Gensler R. J. Rheol 1999;43:359–74.
[22] Gotsis D, Zeevenhoven BLF, Tsenoglou C. J Rheol 2004;48:895–914.
[23] Hu GH, Flat JJ, Lambla M. In: Al-Malaika S, editor. Reactive modifiers for polymers. London: Blackie Academic and Professional; 1997. p. 96–265.
[24] Tzoganakis C, Vlachopoulos J, Hamielec AE. Polym Eng Sci 1989;29:390–6.
[25] Munteanu D. In: Al-Malaika S, editor. Reactive modifiers for polymers. London: Blackie Academic and Professional; 1997. p. 196–265.
[26] Forsyth JC, Baker WE, Russell KE, Whitney RA. J Polym Sci Part A: Polym Chem 1997;35:3517–25.
[27] Spencer M, Parent JS, Whitney RA. Polymer 2003;44:2015–23.
[28] Rust FF. J Am Chem Soc 1957;79:4000–3.
[29] Russell KE, Kelusky EC. J Polym Sci, Part A: Polym Chem 1988;26:2273–80.